Carbohydrate Polymers 75 (2009) 246–250

Contents lists available at ScienceDirect

Carbohydrate Polymers

journal homepage: www.elsevier.com/locate/carbpol

Superhydrophobicity of cellulose triacetate fibrous mats produced by electrospinning and plasma treatment

Young Il Yoon [a], Hyun Sik Moon [b], Won Seok Lyoo [c], Taek Seung Lee [a], Won Ho Park [a,*]

[a] Department of Advanced Organic Materials and Textile System Engineering and BK21 FTIT, Chungnam National University, Gung-dong 220, Yuseong-gu, Daejeon 305-764, Republic of Korea
[b] Reserach Institude of Advanced Materials Chungnam National University, Deajeon, Republic of Korea
[c] Division of Advanced Organic Materials, School of Textiles, Yeungnam University, Gyeongsan 712-749, Republic of Korea

ARTICLE INFO

Article history:
Received 20 May 2008
Received in revised form 27 June 2008
Accepted 1 July 2008
Available online 18 July 2008

Keywords:
Cellulose triacetate (CTA)
Electrospinning
Superhydrophobicity
Plasma
Water contact angle (WCA)

ABSTRACT

Nano/micro-fibrous cellulose triacetate (CTA) mats were prepared by electrospinning a fixed concentration of CTA with different methylene chloride (MC)/ethanol (EtOH) ratios and with various concentrations of CTA at a fixed MC/EtOH 80/20 (v/v) ratio. All of the electrospun CTA mats had a high water contact angle (WCA) compared to the CTA cast film. At a solvent composition of 80/20 (v/v) and 5 wt.% CTA concentration, the CTA mat without plasma treatment had good surface roughness and electrospinning processability, and its WCA was 142°. To further improve its hydrophobicity, the CTA fibrous mat electrospun from the 5 wt.% solution of CTA was treated with a CF_4 plasma for various times. Superhydrophobicity could be obtained after the CF_4 plasma treatment. The WCA of the CTA mat reached as high as 153° after plasma treatment for 60 s.

1. Introduction

It has long been known that lotus leaves show excellent water-repellent properties, and much effort has been made to mimic the superhydrophobicity of the lotus-leaf and to construct a superhydrophobic surface applicable to self-cleaning materials. In 1997, Barthlott revealed the interdependence between the surface roughness, reduced particle adhesion, and water repellency to be the keystone in the self-cleaning mechanism of many biological surfaces (Barthlott & Neinhuis, 1997). The superhydrophobicity of the lotus-leaf is due to the surface roughness caused by the branch-like or protrusion nanostructure on the micropapillae and the low surface energy epicuticular wax (Feng et al., 2003).

The wetting behavior of a solid surface is important for various commercial applications and strongly depends on both the surface energy or chemistry and the surface roughness. It was reported that a superhydrophobic surface with a water contact angle (WCA) higher than 150° could be prepared by the solution method, the sol–gel method, the solidification of an alkyl ketene dimer, the plasma fluorination method, and other methods (Bico, Marzolin, & Quere, 1999; Erbil, Demirel, Avci, & Mert, 2003; Feng et al., 2002; Genzer & Efimenko, 2000; Nakajima, Abe, Hashimoto, & Watanabe, 2000; Nakajima, Fujishima, Hashimoto, & Watanabe, 1999; Onda, Shibuichi, Satoh, & Tsujii, 1996; Shirtcliffe, Hale, Newton, & Perry, 2003; Sun et al, 2003; Teare et al., 2002).

Recently, electrospinning has been reported to be a good and effective method of fabricating micro- to nano-scale fibers from various polymers, such as cellulose acetate (Ding et al., 2006; Han, Son, Youk, Lee, & Park, 2005), polystyrene (Jiang et al., 2004), polybutadiene (Woodward, Schofield, Roucoules, & Badyal, 2003), polycaprolactone (Ma, Mao, Gupta, Gleason, & Rutledge, 2005), for a broad range of applications including membranes, tissue engineering, optical, biosensors, and drug delivery (Sanders, Kloefkorn, Bowlin, Simpson, & Wnek, 2003; Wang et al., 2002; Wnek, Carr, Simpson, & Bowlin, 2003; Zong et al, 2003). Electrospinning is also a unique technology that can produce nonwoven-type mats with a hierarchical micro/nanostructure.

Cellulose triacetate has been widely used in membrane technology because it has good hydrolytic stability and excellent resistance to free chlorine and biodegradation.

Herein, we investigated the preparation and characterization of lotus-leaf-like micro/nanofibrous mats with CTA. CTA fibers were prepared by electrospinning CTA at a fixed concentration with different methylene chloride (MC)/ethanol (EtOH) ratios ranging from 80/20 (v/v) to 100/0 (v/v) and with different concentrations of CTA at a fixed MC/EtOH (80/20) ratio. To improve their hydrophobicity, the CTA fibers electrospun from the 5 wt.% CTA solution at an MC/EtOH ratio of 80/20 were treated with a CF_4 plasma for 0 ~ 300 s. The CTA fibers were characterized by scanning electron

* Corresponding author. Tel.: +82 42 821 6613; fax: +82 42 823 3736.
E-mail address: parkwh@cnu.ac.kr (W.H. Park).

0144-8617/$ - see front matter © 2008 Elsevier Ltd. All rights reserved.
doi:10.1016/j.carbpol.2008.07.015

microscopy (SEM), water contact angle (WCA) and tilting angle (WTA) analyses, X-ray photoelectron spectroscopy (XPS), and atomic force microscopy (AFM).

2. Experimental

2.1. Materials

CTA (Acetyl content = 50 wt.%) was purchased from Aldrich, Co. Ltd. methylene chloride (MC) and ethanol (EtOH) were used as received from Aldrich Co. Ltd.

2.2. Electrospinning

A 5 wt.% CTA solution was prepared in solvent mixtures of MC/EtOH (100/0, 90/10, and 80/20, v/v). CTA solutions with different concentrations ranging from 3 to 9 wt.% were also prepared in a solvent mixture of MC/EtOH (80/20, v/v). The electrospinning needle (ID = 0.495 mm) was connected to a high voltage supply (Chungpa EMT, CPS-40K03) which can generate positive DC voltages of up to 40 kV. The distance between the needle tip and the ground electrode was 10 cm. The applied positive voltage was 10 kV. The CTA solution was delivered via a syringe (20 mL) pump to control the mass flow rate. The mass flow rate of the solution was 5 mL/h. All electrospinning was carried out at room temperature.

2.3. Plasma treatment

CF_4 plasma treatment was carried out for various times with the CTA mat electrospun from the 5 wt.% solution in a chamber ($26 \times 26 \times 10$ cm) connected to a two-stage rotary pump via a liquid nitrogen cold trap with a base pressure of 4×10^{-3} mbar. A L–S matching unit was used to minimize the standing wave ratio (SWR) of the power transmitted from a 13.56 MHz radio frequency generator. Prior to each plasma treatment, the chamber was cleaned using a 50 W air plasma for 30 min. A piece of the CTA mat was then placed in the center of the chamber, followed by evacuation to base pressure. Next, CF_4 gas (99.7% purity) was admitted into the system via a needle valve at a pressure of 0.2 mbar, and the electrical discharge was ignited. Upon the completion of the surface modification, the gas feed was turned off and the chamber vented to the atmosphere.

2.4. Characterization

The morphology and structure of the electrospun CTA fibers were observed on a scanning electron microscope (SEM) (Hitachi S-2350) after gold coating. The WCA and WTA were measured by a DSA 100 drop shape analysis system (Kruss Gmbh). The volume of the water droplet for each measurement was kept at 3×10^{-9} m^3. The XPS spectra of the electrospun CTA mats were recorded on a VG Escalab Mk2 spectrometer equipped with an unmonochromatized Mg-Kα X-ray source (1253.6 eV) and hemispherical analyzer. The photoemitted core level electrons were collected at a fixed takeoff angle (75° with respect to the sample surface) with electron detection in constant analyzer energy (CAE) mode operating at a pass energy of 20 eV. The AFM images were acquired using a Digital Instruments Nanoscope 3 scanning probe microscope. Damage to the tip and sample surface was minimized by employing a Tapping Mode AFM.

3. Results and discussion

3.1. Effect of solvent composition

CTA fibers were prepared by electrospinning from a 5 wt.% solution of CTA with different MC/EtOH ratios ranging from 80/20 (v/v) to 100/0 (v/v). CTA was insoluble in MC/EtOH mixtures with an MC content above 20 vol.%. Selected SEM images are shown in Fig. 1. The CTA fibers electrospun at MC/EtOH ratios of 90/10 and 100/0 had a lot of pores on the surface (Fig. 1b and c). The porous struc-

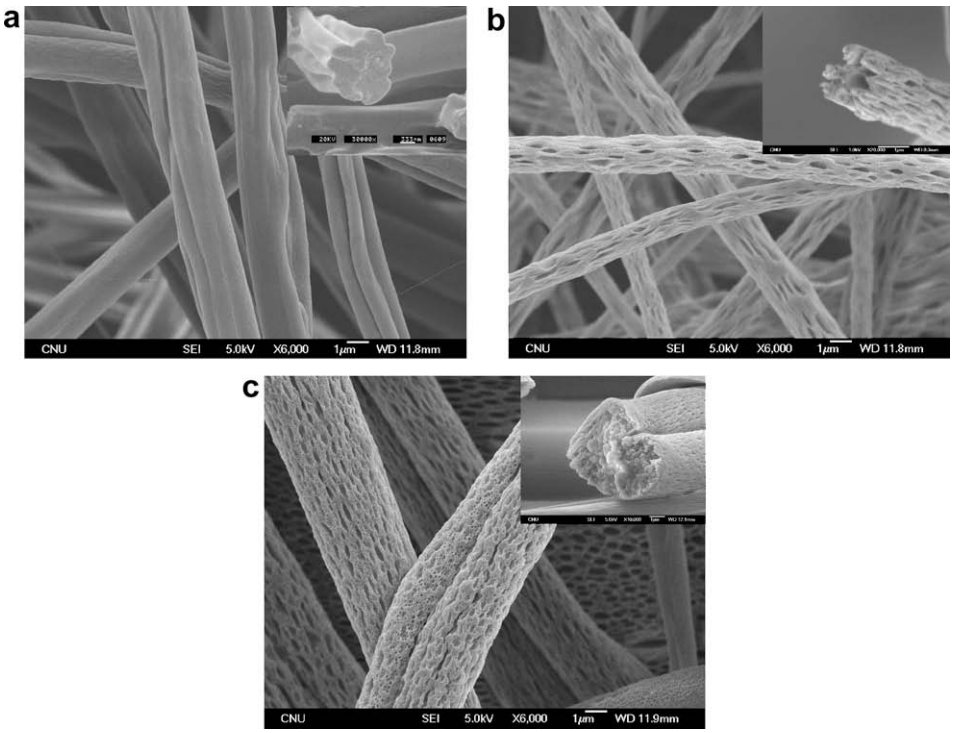

Fig. 1. SEM images of CTA fibers electrospun with different MC/EtOH (v/v) ratios; (a) 80/20, (b) 90/10, and (C) 100/0.

ture was induced by the phase separation resulting from the rapid evaporation of MC (bp = ~40 °C) during the electrospinning process, as reported by Wendorff et al. (Bognitzki et al., 2001). On the other hand, the CTA fibers electrospun at a solvent ratio of 80/20 (v/v) had a non-porous surface and a relatively narrow fiber diameter distribution (Fig. 1a). The CTA fibers were relatively difficult to electrospun at solvent ratios of 90/10 and 100/0 due to the rapid evaporation of MC.

Table 1 presents the WCAs and WTAs of the CTA fibrous mats obtained using different solvent ratios, together with those of the CTA cast film. Compared to the cast film, all of the electrospun mats had much higher WCAs due to their surface roughness. The WCA and WTA values of the electrospun mats were in the ranges of 121 ~ 142° and 12 ~ 19°, respectively, whereas the WCA of the CTA film is 80° (Fig. 2). The CTA fibers electrospun at solvent ratios of 90/10 and 80/20 had higher WCAs because of their relatively low fiber diameter (large surface area of the fiber). Recently, Singh et al. have electrospun superhydrophobic surfaces from poly[bis(2,2,2-trifluoroethoxy)phosphazene] (Singh, Steely, & Allcock, 2005). They found that a decrease in fiber diameter increased the hydrophobicity of these mats to give WCA in the range of 135 ~ 159°. This relationship between the fiber diameter and WCA (hydrophobicity) was consistent with the results in Table 1. The CTA fibers electrospun at a solvent ratio of 90/10 had a porous surface, and those electrospun at a solvent ratio of 80/20 had a unique wrinkled surface. Both porous and wrinkled surfaces can provide the CTA fibrous mats with a high surface area and high WCA. The fiber diameters contribute to the macro-scale roughness between the fibers, while porous, or wrinkled surfaces contribute to the micro-scale roughness within a fiber. From the results in Table 1, it can be seen that the fiber diameter was more important in imparting hydrophobicity to the CTA mats than the surface structure.

3.2. Effect of CTA concentration

CTA fibrous mats were prepared by electrospinning with various concentrations of CTA at a fixed MC/EtOH ratio of 80/20 (v/v). The CTA concentration was varied from 3 to 9 wt.% and the selected SEM images are shown in Fig. 3. All of the CTA fibers had a wrinkled surface and showed a narrow fiber diameter distribution, except for those produced with 3 wt.% CTA. The CTA fibers electrospun from the 3 wt.% solution contained some large beads because of the low concentration of CTA.

Table 1
WCA and WTA of CTA cast film and CTA fibrous mats with various solvent mixtures

CTA (5 wt.%)	Fiber diameter (μm)	WCA (°)	WTA (°)
Fibrous mat, MC/EtOH 80/20 (v/v)	1.7 ± 0.3	141.6 ± 2.2	12.1 ± 1.3
Fibrous mat, MC/EtOH 90/10 (v/v)	1.8 ± 0.5	140.7 ± 0.7	16.1 ± 1.9
Fibrous mat, MC/EtOH 100/0 (v/v)	4.1 ± 1.6	121.5 ± 3.8	17.9 ± 1.9
Cast film	–	80.0 ± 2.0	–

In Table 2, the WCAs and WTAs of the CTA mats electrospun from different CTA concentrations are listed. As the concentration increased from 3 to 9 wt.%, the average fiber diameter increased from 0.23 to 3.41 μm. However, the cross-section of the CTA fibers electrospun with different concentrations had a unique wrinkled structure (Fig. 3). As the CTA concentration increased from 5 to 9 wt.%, the WCA decreased from 142° to 132° and, thus, the WTA increased from 12° to 18°. In the case of the 3 wt.% CTA solution, we could not obtain homogeneous fibrous mats without large beads for the WCA and WTA test.

Considering its good hydrophobicity and electrospinnability, the CTA fibrous mat electrospun with an MC/EtOH ratio of 80/20 (v/v) and 5 wt.% solution was chosen as a good substrate for CF_4 plasma treatment.

3.3. Effect of plasma treatment

To obtain CTA fibrous mats with superhydrophobic surface, plasma treatment by CF_4 gas was employed. Through this plasma treatment, fluorine atoms could be introduced onto the CTA fiber surface, resulting in a decrease in the surface energy of the CTA fibrous mats. The CTA fibers electrospun from the 5 wt.% solution with an MC/EtOH ratio of 80/20 (v/v) were treated with a CF_4 plasma for 0 ~ 300 s. Fig. 4 shows the AFM images of the surface of the CTA mat before and after plasma treatment. As shown in Fig. 4a, the non-treated electrospun CTA mat had a rough surface resembling a lotus-leaf. The WCA of the CTA mat prior to plasma treatment was 142°. The surface roughness of the CTA mat was maintained up to 60 s (Fig. 4b), but when the plasma treatment time was further increased, the surface roughness was reduced due to the etching (collapse) of the protrusion peaks in the surface, due to the excessive plasma treatment (Fig. 4c and d).

Fig. 5a shows the XPS spectra of the CTA mats after plasma treatment. The XPS spectra of the CTA mats subjected to plasma treatment contained a strong peak in the region of 690–700 eV. This peak is characteristic of fluorine 1 s and indicates the presence of fluorocarbons (CF_x) on the CTA mat. The elemental composition after plasma treatment identified by the XPS spectra is shown in Fig. 5b. As shown in Fig. 5b, the fluorine content increased abruptly to ~45% at 60 s and thereafter remained above 40%.

The variations in the WCA and WTA of the CTA mat with the plasma treatment time are shown in Fig. 6. The CTA fibrous mats had a maximum WCA of 153° and a minimum WTA of 4° at 60 s, indicating their superhydrophobicity. As the plasma treatment time was further increased from 60 to 300 s, the WCA of the CTA mats gradually decreased, because the surface etching effect

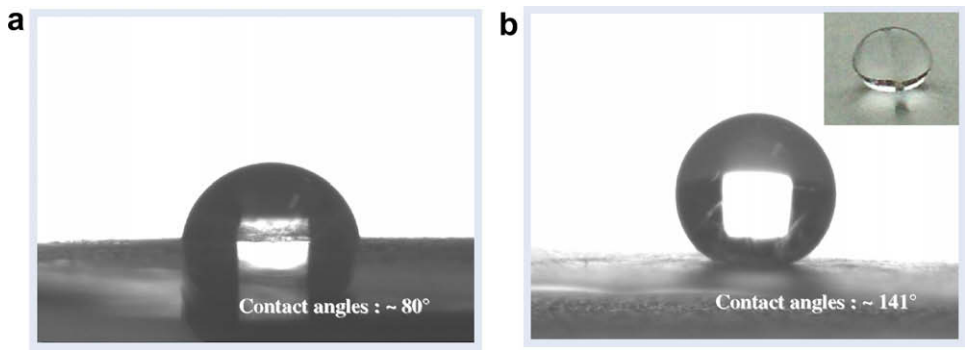

Fig. 2. Water droplets on CTA cast film (a) and CTA fibrous mat (b).

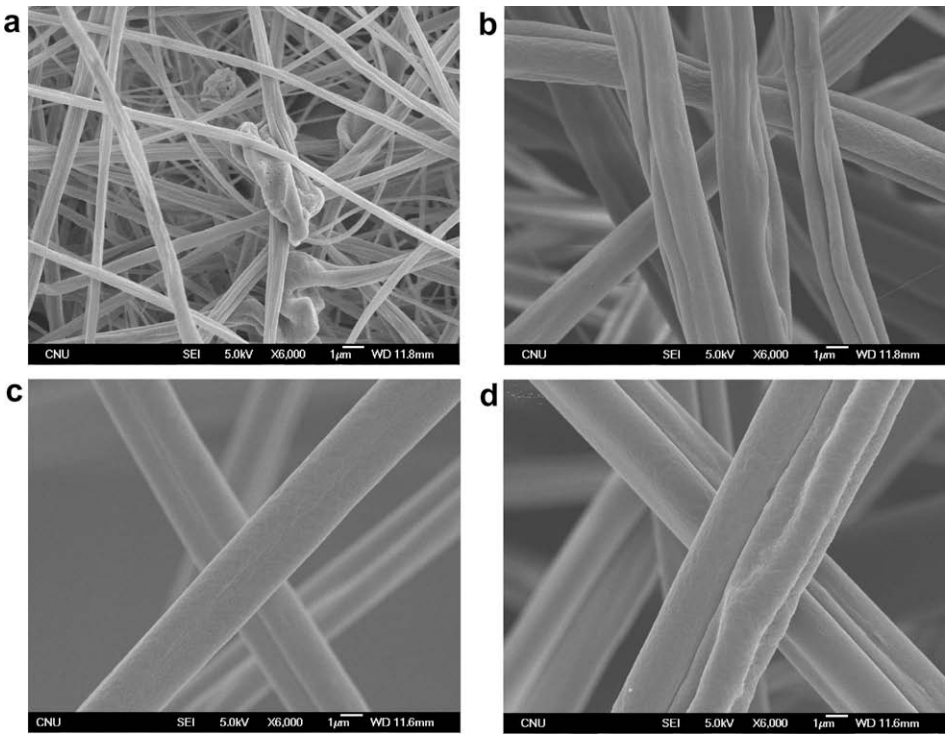

Fig. 3. SEM images of CTA fibers electrospun with various CTA concentrations; (a) 3 wt.%, (b) 5 wt.%, (c) 7 wt.%, and (d) 9 wt.%.

Table 2
WCA and WTA of CTA fibrous mats with various CTA solutions

Concentration (wt.%)	Fiber diameter (μm)	WCA (°)	WTA (°)
3	0.2 ± 0.1	–	–
5	1.7 ± 0.3	141.6 ± 2.2	12.1 ± 1.3
7	2.0 ± 0.4	136.2 ± 1.9	18.3 ± 0.6
9	3.4 ± 0.7	132.0 ± 1.3	18.5 ± 0.3

caused by excessive plasma treatment became dominant, resulting in a decrease in the surface roughness and fluorine content.

4. Conclusions

Superhydrophobic CTA fibrous mats were fabricated via a two-stage process; electrospinning to generate surface roughness and

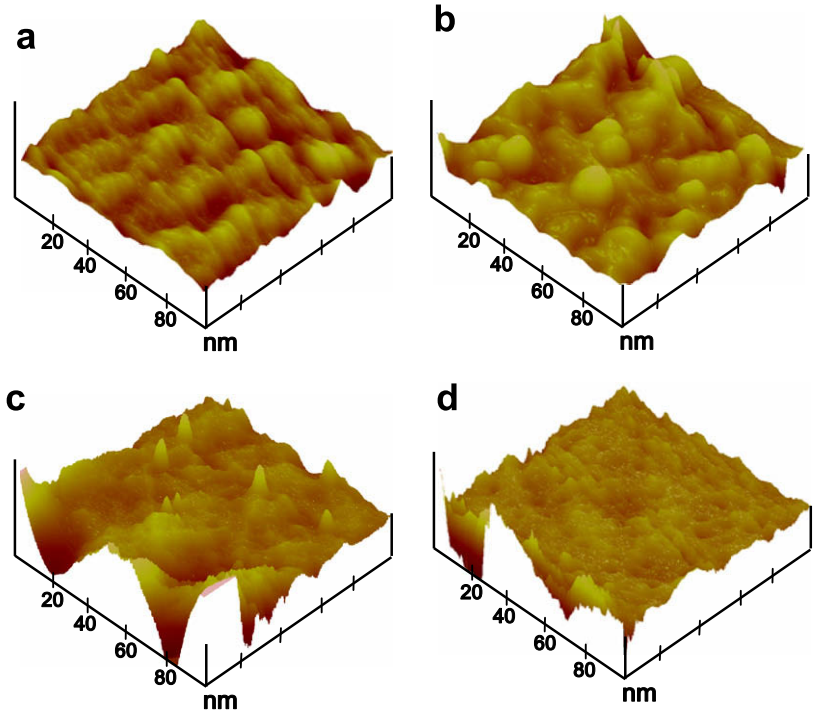

Fig. 4. AFM images of CTA fibrous mats with various plasma treatment times; (a) 0 s, (b) 60 s, (c) 180 s, and (d) 300 s.

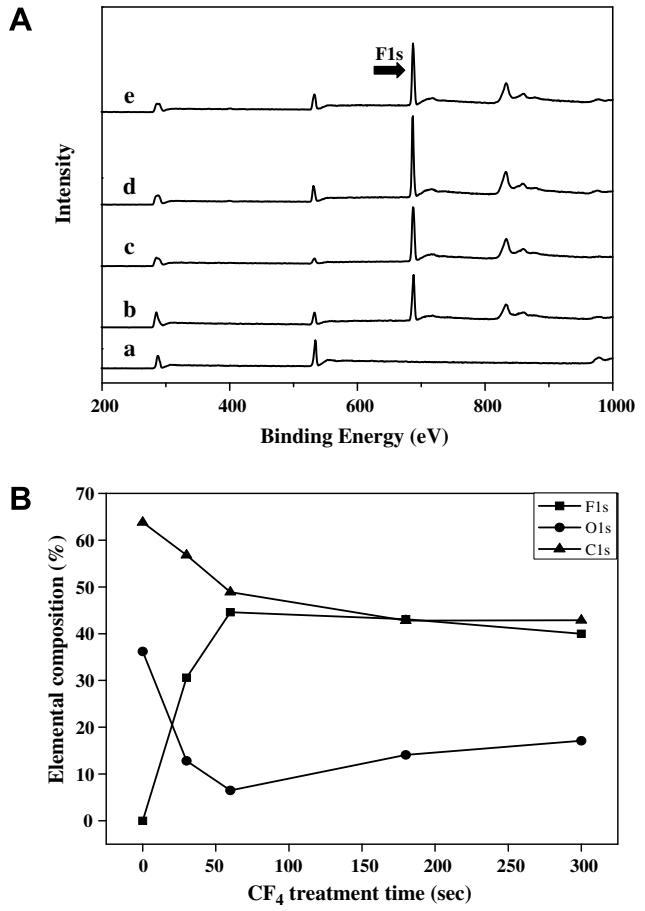

Fig. 5. XPS spectra (A) and elemental compositions (%) (B) of electrospun CTA mat with various plasma treatment times; (a) 0 s, (b) 30 s, (c) 60 s, (d) 180 s, and (e) 300 s.

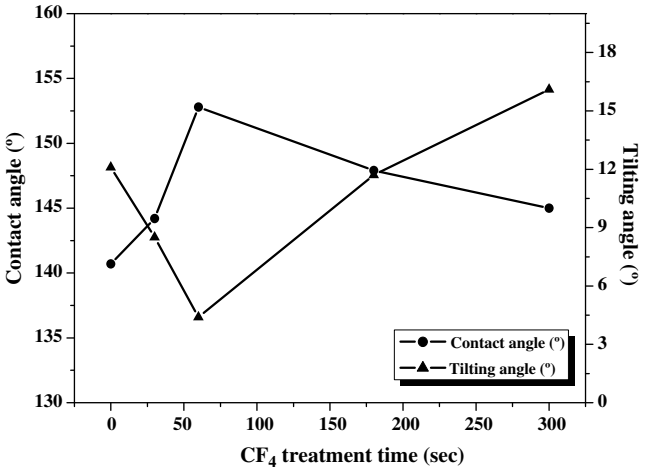

Fig. 6. Variation in WCA and WTA of CTA fibrous mats with plasma treatment time.

CF_4 plasma treatment to reduce the surface energy. For this purpose, CTA fibrous mats were prepared by electrospinning a fixed concentration of CTA with different MC/EtOH solvent ratios ranging from 80/20 to 100/0 (v/v) and with various concentrations of CTA at a fixed solvent ratio of 80/20 (v/v). All of the electrospun CTA mats showed a high WCA compared to the CTA cast film. The CTA fibrous mat electrospun from 5 wt.% CTA showed a maximum WCA of 142° due to its appropriate surface roughness. To obtain a superhydrophobic surface, the CTA fibrous mat electrospun from 5 wt.% CTA solution with an 80/20 (v/v) solvent mixture was treated with a CF_4 plasma for various times. After plasma treatment for 60 s, the WCA and WTA of the CTA fibrous mat reached as high as 153° and as low as 4°, respectively, indicating that the CTA surface is superhydrophobic. Further plasma treatment reduced the surface roughness of the CTA mat, and thus decreased its WCA. The extremely high hydrophobicity of the CTA fibrous mat after plasma treatment for 60 s was attributed to the inherent surface roughness and surface fluorination.

Acknowledgments

This work was financially supported by Regional Technology Innovation Program of the Ministry of Commerce, Industry, and Energy (Grant No. RTI04-01-04).

References

Barthlott, W., & Neinhuis, C. (1997). Purity of the sacred lotus, or escape from contamination in biological surfaces. *Planta, 202*, 1–8.
Bico, J., Marzolin, C., & Quere, D. (1999). Pearl drops. *Europhysics Letters, 47*, 220–226.
Bognitzki, M., Czado, W., Frese, T., Schaper, A., Hellwig, M., Steinhart, M., et al. (2001). Nanostructured fibers via electrospinning. *Advanced Materials, 13*, 70–72.
Ding, B., Li, C., Hotta, Y., Kim, J., Kuwaki, O., & Shiratori, S. (2006). Conversion of an electrospun nanofibrous cellulose acetate mat from a super-hydrophilic to super-hydrophobic surface. *Nanotechnology, 17*, 4332–4339.
Erbil, H. Y., Demirel, A. L., Avci, Y., & Mert, O. (2003). Transformation of a simple plastic into a superhydrophobic surface. *Science, 299*, 1377–1380.
Feng, L., Li, S., Li, Y., Li, H., Zhang, L., Zhai, J., et al. (2002). Super-hydrophobic surfaces: From natural to artificial. *Advanced Materials, 14*, 1857–1860.
Feng, L., Song, Y. L., Zhai, J., Liu, B., Xu, J., Jiang, L., et al. (2003). Creation of a superhydrophobic surface from an amphiphilic polymer. *Angewandte Chemie (International Edition), 42*, 800–802.
Genzer, J., & Efimenko, K. (2000). Creating long-lived superhydrophobic polymer surfaces through mechanically assembled monolayers. *Science, 290*, 2130–2133.
Han, S. O., Son, W. K., Youk, J. H., Lee, T. S., & Park, W. H. (2005). Ultrafine porous fibers electrospun from cellulose triacetate. *Materials Letters, 59*, 2998–3001.
Jiang, L., Zhao, Y., & Zhai, J. (2004). A lotus-leaf-like Superhydrophobic surface. A porous microsphere/nanofiber composite film prepared by electrohydrodynamics. *Angewandte Chemie (International Edition), 33*, 4338–4341.
Ma, M., Mao, Y., Gupta, M., Gleason, K., & Rutledge, G. C. (2005). Superhydrophobic fabrics produced by electrospinning and chemical vapor deposition. *Macromolecules, 38*, 9742–9748.
Nakajima, A., Abe, K., Hashimoto, K., & Watanabe, T. (2000). Preparation of hard super-hydrophobic films with visible light transmission. *Thin Solid Films, 376*, 140–143.
Nakajima, A., Fujishima, A., Hashimoto, K., & Watanabe, T. (1999). Preparation of transparent superhydrophobic Boehmite and silica films by sublimation of aluminum acetylacetonate. *Advanced Materials, 11*, 1365–1368.
Onda, T., Shibuichi, S., Satoh, N., & Tsujii, K. (1996). Super-water-repellent fractal surfaces. *Langmuir, 12*, 2125–2127.
Sanders, E. H., Kloefkorn, R., Bowlin, G. L., Simpson, D. G., & Wnek, G. E. (2003). Two-phase Electrospinning from a single electrified jet: Microencapsulation of aqueous reservoirs in poly(ethylene-co-vinyl acetate) fibers. *Macromolecules, 36*, 3803–3805.
Shirtcliffe, N. J., Hale, G., Newton, M. I., & Perry, C. C. (2003). Intrinsically superhydrophobic organosilica sol-gel foams. *Langmuir, 19*, 5626–5631.
Singh, A., Steely, L., & Allcock, H. R. (2005). Poly[bis(2,2,2-trifluoroethoxy)phosphazene] superhydrophobic nanofibers. *Langmuir, 21*, 11604–11607.
Sun, T., Wang, G., Liu, H., Feng, L., Jiang, L., & Zhu, D. (2003). Control over the wettability of an aligned carbon nanotube film. *Journal American Chemical Society, 125*, 14996–14997.
Teare, D. O. H., Spanos, C. G., Ridley, P., Kinmond, E. J., Roucoules, V., Badyal, J. P. S., et al. (2002). Pulsed plasma deposition of super-hydrophobic nanospheres. *Chemistry of Materials, 14*, 4566–4571.
Wang, X. Y., Drew, C., Lee, S. H., Senecal, K. J., Kumar, J., & Samuelson, L. A. (2002). Electrospun nanofibrous membranes for highly sensitive optical sensors. *Nano Letters, 2*, 1273–1275.
Wnek, G. E., Carr, M. E., Simpson, D. G., & Bowlin, G. L. (2003). Electrospinning of nanofiber fibrinogen structures. *Nano Letters, 3*, 213–216.
Woodward, I., Schofield, W. C. E., Roucoules, V., & Badyal, J. P. S. (2003). Super-hydrophobic surfaces produced by plasma fluorination of polybutadiene films. *Langmuir, 19*, 3432–3438.
Zong, X. H., Ran, S. F., Kim, K. S., Fang, D. F., Hsiao, B. S., & Chu, B. (2003). Structure and morphology changes during in vitro degradation of electrospun poly(glycolide-co-lactide) nanofiber membrane. *Biomacromolecules, 4*, 416–423.